crystals

MDPI

Article

Optical and Thermoelectric Properties of Surface-Oxidation Sensitive Layered Zirconium Dichalcogenides $ZrS_{2-x}Se_x$ (x=0, 1, 2) Crystals Grown by Chemical Vapor Transport

Thalita Maysha Herninda and Ching-Hwa Ho *

Graduate Institute of Applied Science and Technology, National Taiwan University of Science and Technology, Taipei 106, Taiwan; chho@ mail.ntust.edu.tw

* Correspondence: chho@ mail.ntust.edu.tw; Tel.: +886-2-27303772; Fax: +886-2-27303733

Received: 11 April 2020; Accepted: 20 April 2020; Published: date

Supporting Information

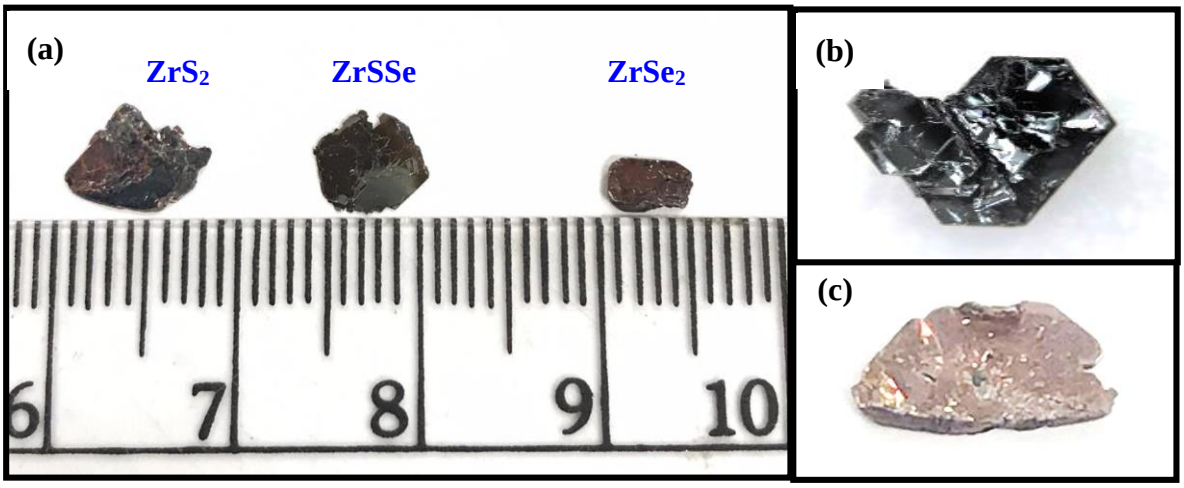

Figure S1. (**a**) Crystal morphology of *c*-plane layered $ZrS_{2-x}Se_x$ (x = 0, 1, and 2). (**b**) Fresh-surface $ZrSe_2$ with removing the outer layer to present dark and shiny surface. (**c**) When the $ZrSe_2$ was oxidized, the color will change into pink red and white color on its surface.

Table S1. The comparison of lattice constants of $ZrS_{2-x}Se_x$ obtained by XRD and TEM measurements.

	Material	XRD *a*-xis (Å)	XRD *c*-axis (Å)	TEM *a*-axis (Å)
x=0	ZrS_2	3.656	5.818	3.651
x=1	$ZrSSe$	3.690	5.980	3.687
x=2	$ZrSe_2$	3.768	6.101	3.769

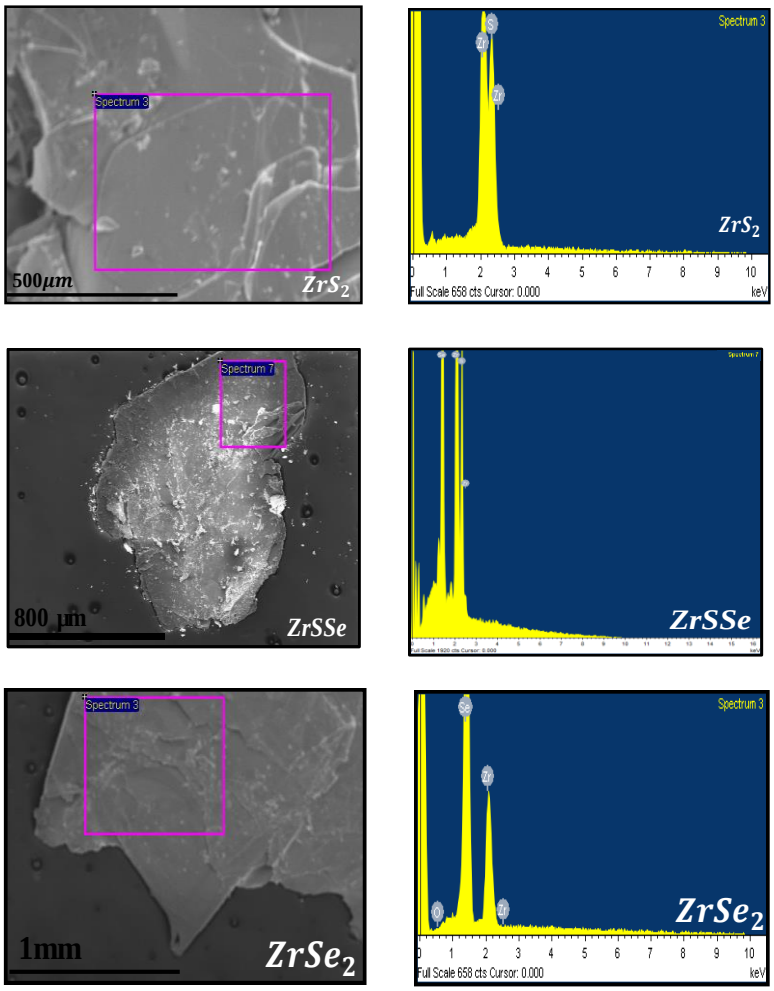

Material	$ZrSe_2$ Oxidized			ZrSSe Oxidized				ZrS_2 Oxidized		
	Zr	Se	O	Zr	Se	S	O	Zr	S	O
Ideal Atomic (%)	33.33	66.66	-	33.33	33.33	33.33	-	33.33	66.66	-
Atomic (%)	33.31	32.62	34.07	34.02	26.31	26.32	13.35	34.09	50.18	15.73

Material	$ZrSe_2$ Fresh			ZrSSe Fresh				ZrS_2 Fresh		
	Zr	Se	O	Zr	Se	S	O	Zr	S	O
Ideal Atomic (%)	33.33	66.66	-	33.33	33.33	33.33	-	33.33	66.66	-
Atomic (%)	34.01	65.79	0.2	33.88	33.68	32.29	0.15	34.12	65.71	0.17

Figure S2. Energy Dispersive X-ray (EDX) analysis of $ZrS_{2-x}Se_x$ (x = 0, 1, and 2) after oxidation. The upper table shows atomic percentage of Zr, S, Se, and O that were analyzed using EDX spectra of oxidized surface. The lower table shows the stoichiometric content of fresh surface after the exfoliation of the sample surface. All the samples with new surface show chalcogen deficiency and a little bit oxygen existed in the $ZrS_{2-x}Se_x$ (x = 0, 1, and 2) series.

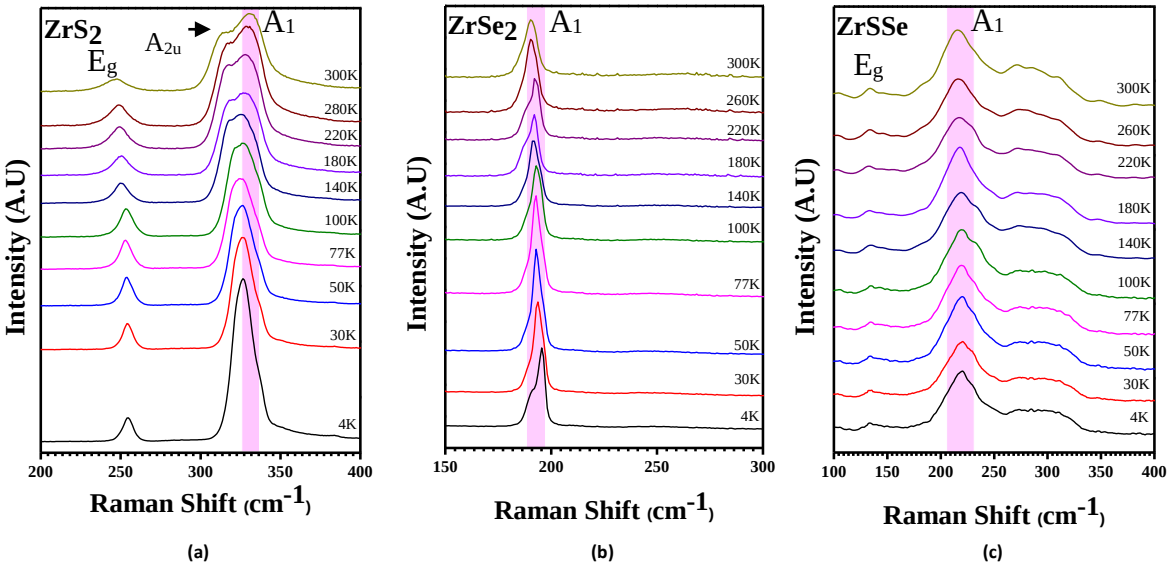

Figure S3. Temperature-dependent Raman spectra of (**a**) ZrS_2, (**b**) $ZrSe_2$, and (**c**) ZrSSe. The main peaks (A_{1g}) were highlighted by purple bars. It shows reduction in peak wavenumber from 4 to 300 K for all the $ZrS_{2-x}Se_x$ samples. The peak of E_g mode in ZrS_2 and ZrSSe also revealed similar temperature-energy shift behavior with that of A_{1g} mode owing to the shrinkage of the ZrX_2 (X = S, Se) lattice from 300 down to 4 K.

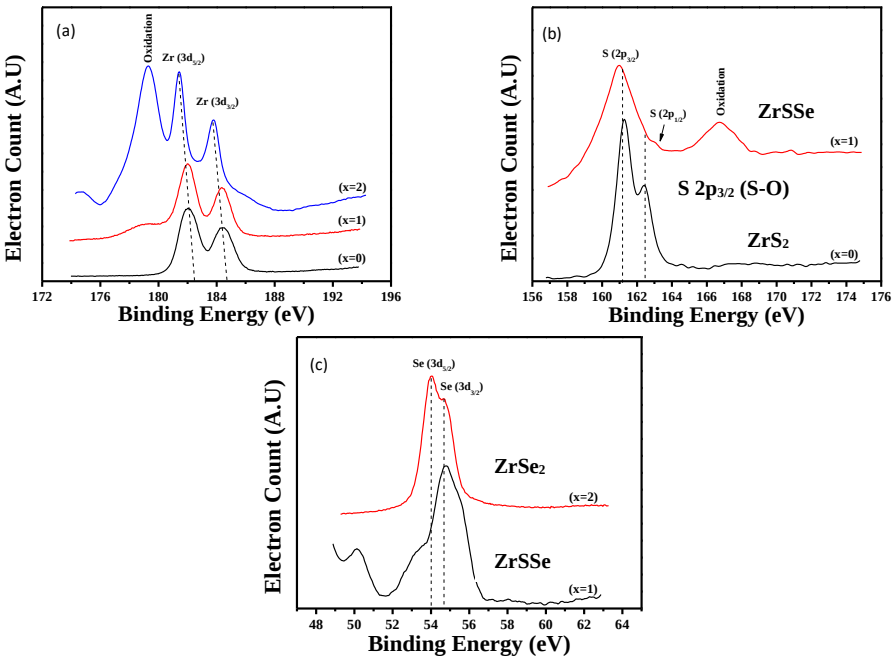

Figure S4. The XPS spectra of (**a**) Zr $3d_{3/2}$ and Zr $3d_{5/2}$, (**b**) S $2p_{3/2}$ and S $2p_{1/2}$, and (**c**) Se $3d_{5/2}$ and Se $3d_{3/2}$ in $ZrS_{2-x}Se_x$ (x = 0, 1, and 2). The Zr $3d_{3/2}$ and Zr $3d_{5/2}$ peaks shift to lower binding energy with the Se content is increased and one additional oxidation peak at ~179 eV (Zr 3*d* in sub-oxide) (see Reference S1) is observed in $ZrSe_2$ in (**a**). For the S 2*p* and Se 3*d* orbitals, they still reveal redshift as the Se content is increased. The oxidation effect can also be observed in one oxidation peak near 167 eV (i.e., S-O bond) in ZrSSe and ZrS_2 in (**b**).

Table S2. Resistivity and Hall measurement results at 300 K.

	ZrS_2	$ZrSSe$	$ZrSe_2$
Resistivity (Ω.cm)	0.25	0.0211	0.0058
Hall Coefficient ($C \cdot cm^{-3}$)	15.42	3.929	2.12
Type	n	n	n
Concentration (cm^{-3})	4.05×10^{17}	1.6×10^{18}	2.9×10^{18}
Mobility ($cm^2/V \cdot Sec$)	61.78	186.17	353.33

Supporting Information References

S1. Bespalov, M. Datler, S. Buhr, W. Drachsel, G. Rupprechter, Y. Suchorski, Ultramicroscopy **159**, 147 (2015).